Spin-Flip Transitions Induced by Time-Dependent Electric Fields in Surfaces with Strong Spin-Orbit Interaction

Julen Ibañez-Azpiroz,[1,2] Asier Eiguren,[1,2] E. Ya. Sherman,[3,4] and Aitor Bergara[1,2,5]

[1]*Materia Kondentsatuaren Fisika Saila, University of Basque Country UPV-EHU, 48080 Bilbao, Euskal Herria, Spain*
[2]*Donostia International Physics Center (DIPC), Paseo Manuel de Lardizabal 4, 20018 Donostia/San Sebastian, Spain*
[3]*Department of Physical Chemistry, University of Basque Country UPV-EHU, 48080 Bilbao, Euskal Herria, Spain*
[4]*IKERBASQUE Basque Foundation for Science, 48011 Bilbao, Bizkaia, Spain*
[5]*Centro de Física de Materiales CFM—Materials Physics Center MPC, Centro Mixto CSIC-UPV/EHU, Edificio Korta, Avenida de Tolosa 72, 20018 Donostia, Basque Country, Spain*

(Received 10 July 2012; published 9 October 2012)

We present a comprehensive theoretical investigation of the light absorption rate at a Pb/Ge(111) $-\beta\sqrt{3}\times\sqrt{3}R30°$ surface with strong spin-orbit coupling. Our calculations show that electron spin-flip transitions cause as much as 6% of the total light absorption, representing 1 order of magnitude enhancement over Rashba-like systems. Thus, we demonstrate that a substantial part of the light irradiating this nominally nonmagnetic surface is attenuated in spin-flip processes. Remarkably, the spin-flip transition probability is structured in well-defined hot spots within the Brillouin zone, where the electron spin experiences a sudden 90° rotation. This mechanism offers the possibility of an experimental approach to the spin-orbit phenomena by optical means.

DOI: 10.1103/PhysRevLett.109.156401 PACS numbers: 71.70.−d, 72.25.Rb, 73.21.−b

Understanding electron spin transport and spin relaxation in quasi-two-dimensional (2D) systems is of capital importance due to both fundamental reasons and the potential technological applications. The spin-orbit (SO) interaction is the most prominent relativistic effect leading to the fascinating phenomena recently observed in 2D systems, such as the quantum spin Hall effect [1,2]. An experimentally accessible spin degree of freedom offers a new route for the emergent field of spintronics, where the main features of charge dynamics are strongly influenced by the spin-related effects [3,4]. The technical possibility of spin manipulation and control by means of an applied bias voltage is strongly supported by recent investigations on a variety of semiconducting alloy samples [5–7].

However, a strong SO coupling cannot be achieved in conventional semiconductors where the spin splitting of conduction electrons is limited to a few meV at most. In contrast, the relativistic effects completely dominate the electronic structure of many heavy-element surface materials and overlayers [8]. The reason lies in the breaking up of the inversion symmetry and the associated gradient of the effective one-electron potential introduced at the interface. These effects lead to extraordinarily large (100–500 meV) spin splittings among the so-called Shockley-type surface states, as it was first observed in the free electron-like Au(111) noble metal surface [9]. This system is regarded as a prototype of the standard Rashba model [10,11]. Considering the general form of the SO interaction in the nonrelativistic limit,

$$\hat{H}_{\mathrm{SO}} = -\frac{\hbar e}{4m^2c^2}\hat{\boldsymbol{\sigma}}\cdot(\mathbf{k}\times\boldsymbol{\nabla}V(\mathbf{r})), \tag{1}$$

the Rashba SO coupling is recovered by taking the gradient of the effective one-electron potential $V(\mathbf{r})$ as a constant and completely surface perpendicular. This model produces an entirely isotropic result, with a simple linear spin splitting of the two spin sub-bands with chiral spin polarization. However, many heavy-element adlayer or even clean surface materials, such as Bi(110) [12], $1\times1H/W(110)$ [13], Au/Si(557) [14], Bi/Si(111) [15,16], or Tl/Si(111) [17–19], exhibit large anisotropic SO interaction, inducing complex spin textures that considerably deviate from the free electronlike picture of the Rashba model.

In this Letter, we investigate electrically induced spin-flip excitations on the Pb/Ge(111) $-\beta\sqrt{3}\times\sqrt{3}R30°$ surface ($\sqrt{3}$Pb/Ge(111)), considering the full spinor structure of the electron states within the *ab initio* density functional theory. The goal is to understand and quantify the striking mechanism leading to spin-flip transitions out of a purely electric perturbation in a nonmagnetic material. This system presents two well-defined spin-split surface states crossing the Fermi level, while the bulk substrate remains semiconducting. Thus, we face a problem involving a completely spin-polarized 2D electron gas that is essentially decoupled from the bulk, i.e., an optimum scenario for studying surface spin-flip transitions [20]. It is noteworthy that the strength of the SO interaction associated to the Pb atoms is 2 orders of magnitude larger (≈ 300 meV) than in semiconductor quantum wells. Moreover, the Pb overlayer includes strong anisotropic gradients in the surface ionic potential, giving rise to a fast variation of the noncollinear spin polarization in momentum space, which critically enhances the spin-flip transition probability.

The spin manipulation in 2D systems [21] is accessible via the electric-dipole spin resonance mechanism, which couples the spin-dependent electron velocity to externally applied fields [22]. At surfaces, the different spin-split sub-bands are connected through interband transitions that flip the electron spin [23]. A detailed analysis of these processes will provide valuable information on the spin dynamics of the system, thus making the first-principles approach imperative. Simplified tight-binding Rashba-like models, although very useful for understanding the basic physics [24], appear to be not realistic enough to account for the material-specific details that determine electromagnetic responses.

Let us consider the interaction of an electron with an external time-dependent electric field of frequency ω. Within the electric dipole approximation valid for a small momentum transfer $\mathbf{q} \to 0$, the interaction Hamiltonian is given by [22,23]

$$\hat{H}_{\text{int}}(t) = -\frac{e}{c}\hat{\mathbf{v}} \cdot \mathbf{A}_{\text{ext}}(t), \tag{2}$$

where $\mathbf{A}_{\text{ext}}(t) = \mathbf{A}_0 \cos\omega t$ is the external vector potential associated to the electric field $\mathbf{E}_{\text{ext}}(t) = \mathbf{E}_0 \sin\omega t$ with $\mathbf{E}_0 = \mathbf{A}_0\omega/c$, and $\hat{\mathbf{v}}$ is the electron velocity operator. In systems with SO coupling, besides the canonical contribution $\hat{\mathbf{p}}/m$, the velocity operator includes an additional spin-dependent term that emerges as the main factor responsible for spin-flip transitions [23].

Within the first-order perturbation theory, the transition rate associated to spin-flip excitations between spin-split surface states S and S' due to photon absorption (term $\mathbf{A}_0 e^{-i\omega\cdot t}/2$) can be derived from the Fermi golden rule,

$$\gamma_{SS'}(\omega) = \frac{2\pi}{\hbar}\int_{SBZ}(f(\epsilon_{S\mathbf{k}}) - f(\epsilon_{S'\mathbf{k}}))|M_{SS'}(\mathbf{k})|^2 \times \delta(\epsilon_{S\mathbf{k}} - \epsilon_{S'\mathbf{k}} - \hbar\omega)\frac{d^2k}{(2\pi)^2}. \tag{3}$$

The integral is taken over the surface Brillouin zone, $f(\epsilon_{i,\mathbf{k}})$ and $\epsilon_{i,\mathbf{k}}$ represent the Fermi-Dirac distribution and a surface state eigenvalue, respectively, and $M_{SS'}(\mathbf{k})$ is the interband matrix element

$$M_{SS'}(\mathbf{k}) = -\frac{e\mathbf{A}_0}{2c} \cdot \langle \Psi_{S\mathbf{k}}|\hat{\mathbf{v}}|\Psi_{S'\mathbf{k}}\rangle. \tag{4}$$

As shown above, $\Psi_{i\mathbf{k}}(\mathbf{r})$ denotes the single-particle Bloch spinor wave function associated to a surface state.

Because of the inherent phase indeterminacy of the Bloch states in $\mathbf{k}$-space, the matrix elements of the velocity operator require a special treatment [25]. Following the approach presented in Ref. [26], we expressed $M_{SS'}(\mathbf{k})$ in Eq. (4) in terms of the so-called maximally localized Wannier functions [27]. In this way, the matrix elements entering Eq. (3) are maximally smooth and thus suitable for any interpolation procedure within the Brillouin zone. The Wannier functions were generated considering the entire structure of *ab initio* spinor wave functions obtained within the noncollinear DFT formalism [28–30].

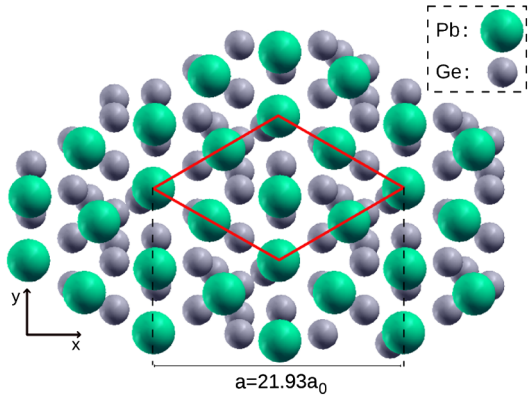

FIG. 1 (color online). Top view of the $\sqrt{3}$Pb/Ge(111) surface [35]. The small (gray) spheres symbolize the Ge substrate layers, whereas the big (green) spheres represent the Pb surface monolayer. The solid (red) parallelogram indicates surface unit cell.

The exchange-correlation energy was approximated using standard LDA-PZ parametrization [31] and the 2×2 norm-conserving fully relativistic pseudopotential approach [30,32]. The ground-state self-consistent cycle was performed considering the usual Monckhorst-Pack mesh corresponding to a 27×27 grid. We employed a very fine 200×200 mesh, considering the standard Wannier interpolation procedure for all the ingredients entering Eq. (3) [26,27], in order to reliably account for the details close to the Fermi level [26].

Figure 1 shows the $\sqrt{3}$Pb/Ge(111) surface (Fig. 1), which was simulated using a repeated slab technique containing 14 Ge layers. The Pb monolayer was included only in one side of the slab, while the other (bare) Ge(111) surface was covered by a hydrogen adlayer in order to saturate the dangling bonds. We also analyzed the Au(111) metal surface, considering a 22 Au layer slab. In both systems, a full geometry optimization was performed until all the atomic forces exerted on individual atoms were negligibly small ($< 10^{-4}$ Ry a.u.$^{-1}$).

Figure 2 shows the calculated band structure of the Pb/Ge(111)$\sqrt{3}$ surface. While a scalar relativistic calculation shows a single spin-degenerate surface band crossing the Fermi level, fully relativistic calculations present two spin-polarized surface bands, labeled as S and S'. SO interaction has a huge impact on the electron structure close to the the Fermi level, such that this term cannot be treated perturbatively. Its contribution is even more important than some nonrelativistic DFT terms such as the exchange-correlation energy. In this context, the SO interaction completely determines the metallic character of the S and S' surface states. These exist as surface states only outside the area close to the $\overline{\Gamma}$ point, where S and S' become resonances entering the bulk projection (continuum in Fig. 2). Outside this region, the splitting is in overall of the order of 100 meV, reaching a maximum of 300 meV near the high symmetry point $\overline{M}$. The calculated

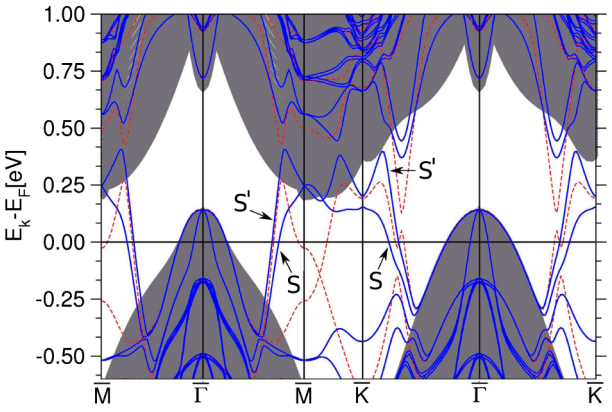

FIG. 2 (color online). Electron band structure of the $\sqrt{3}$Pb/Ge(111) surface. The scalar and fully relativistic bands are represented by dashed (red) and solid thick (blue) lines, respectively. The continuous background is the bulk band projection. The fully relativistic metallic surface states are labeled as S and S'.

Fermi wave vectors along the high symmetry direction $\overline{\Gamma}\,\overline{\mathrm{M}}$, $k_F^S \simeq 0.41$ Å^{-1} and $k_F^{S'} \simeq 0.37$ Å^{-1} are in very good agreement with recent angle-resolved photoemission spectroscopy experiments reporting $k_F^S = 0.40$ Å^{-1} and $k_F^{S'} = 0.36$ Å^{-1} [20].

A characteristic feature emerging from the SO interaction at surfaces is the momentum-dependent spin polarization,

$$\mathbf{m}_n(\mathbf{k}) = \int \Psi^*_{n\mathbf{k}}(\mathbf{r})\hat{\boldsymbol{\sigma}}\Psi_{n\mathbf{k}}(\mathbf{r})d^3r, \qquad (5)$$

where n is the band index. In Figs. 3(a) and 3(b) we present the calculated spin polarization for the S and S' surface states in the entire Brillouin zone. These figures demonstrate that the S and S' states are spin polarized in almost the opposite direction, in agreement with recent spin-resolved angle-resolved photoemission spectroscopy measurements [20]. The negligible spin polarization observed around $\overline{\Gamma}$ is consistent with the overlap of the surface bands with the bulk projection (see Fig. 2). In this area, the electron states become resonances with a large penetration; thus, any surface effect such as the enhancement of the SO interaction is almost completely absent.

The anisotropic character of the SO interaction is evidenced by the highly noncollinear structure of the calculated spin polarization for S and S'. On one hand, we observe that the spin of each surface state is mainly polarized along the surface perpendicular direction, a phenomenon that extends to a significant area around the high symmetry points $\overline{\mathrm{M}}$ and $\overline{\mathrm{M}}'$. Such an important contribution of out-of-plane magnetization is a consequence of the strong in-plane gradients of the ionic potential, as reported in the Tl/Si(111) surface [17–19]. On the other hand, our calculations further identify an important area of almost pure in-plane circular spin polarization for each state around the high symmetry point $\overline{\mathrm{K}}$.

Figure 3(c) shows the results for the calculated spin-flip transition probability $P_{SS'}(\mathbf{k}) \equiv |M_{SS'}(\mathbf{k})|^2/|\mathbf{A}_0|^2$ for an R circularly polarized external field, $\mathbf{A}_0 = A_0(\hat{\mathbf{x}} + i\hat{\mathbf{y}})/\sqrt{2}$. The results for other polarizations, although slightly different, do not substantially modify our general conclusions. We deduce from Fig. 3(c) that the spin-flip transition probability is negligible around the $\overline{\Gamma}$ point. This is consistent with Eq. (5) since the surface states are spin-degenerate here; [26] therefore, SO driven effects such as the spin-flip excitations are weak. On the other hand, the most important message of Fig. 3(c) is the extreme localization of the spin-flip transition probability in hot spots

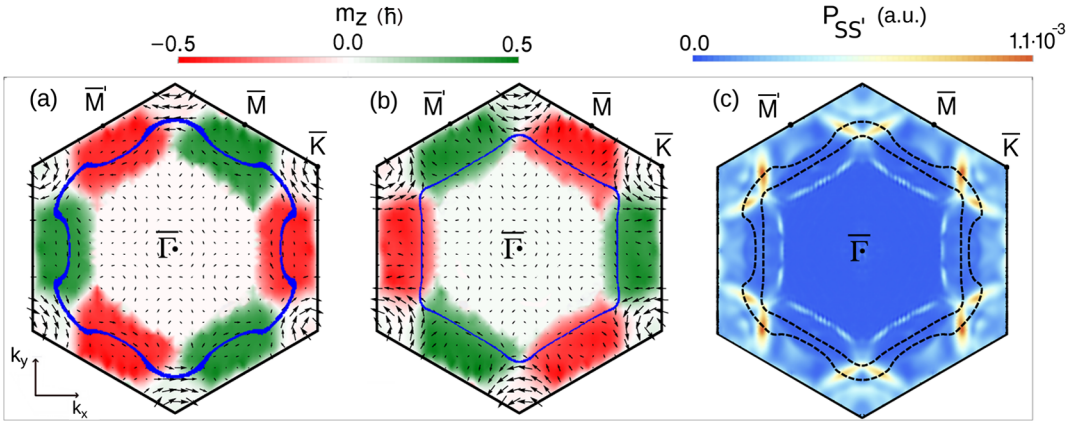

FIG. 3 (color online). (a) and (b) Momentum-dependent spin-polarization structures associated to the S and S' surface states, respectively. Arrows represent the in-plane spin-polarization component, whereas the background indicates the surface perpendicular component of the magnetization, $m_z(\mathbf{k})$. The Fermi surface of each state is indicated by solid (blue) lines. (c) Spin-flip transition probability associated to the S and S' surface states for R-circularly polarized light. The Fermi surface is indicated by the dashed (black) lines.

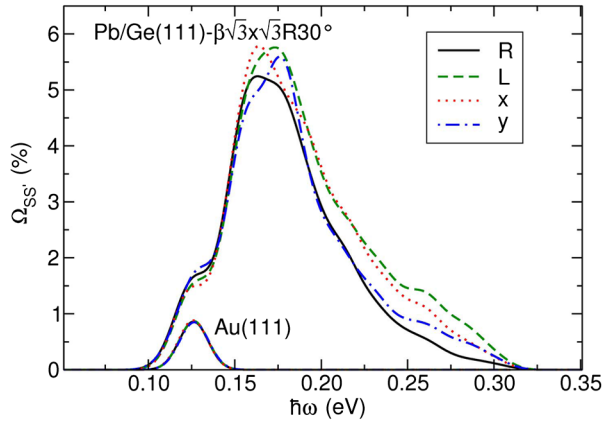

FIG. 4 (color online). Calculated spin-flip absorption rate in $\sqrt{3}$Pb/Ge(111) and Au(111). The solid (black), dashed (green), dotted (red), and dashed-doted (blue) lines represent the results corresponding to the R and L circularly polarized and the x and y linearly polarized lights, respectively. Note that the absorption rate for $\sqrt{3}$Pb/Ge(111) depends on the light polarization, while in Au(111) it is practically polarization independent.

close to the high symmetry point $\overline{\mathrm{K}}$. A careful comparison of Figs. 3(a) and 3(b) with Fig. 3(c) reveals that the hot spots are localized in the boundaries separating the surface-perpendicular and surface-parallel spin-polarized regions in the Brillouin zone. This feature is fully consistent with Eq. (4) since the velocity operator introduces a $\mathbf{k}$-space derivative [25,26], which effectively measures the variation of the entire wave function and spin polarization through Eq. (5). Note that this singular effect is completely absent in Rashba-like systems exhibiting a smooth behavior of spin polarization [9–11].

The light absorption rate associated to surface spin-flip excitations is given by the following expression:

$$\Omega_{SS'}(\omega) = \frac{\hbar\omega \cdot \gamma_{SS'}(\omega)}{W}. \tag{6}$$

Here, $\gamma_{SS'}(\omega)$ is the spin-flip transition rate [Eq. (3)], $\hbar\omega$ the energy of the external field, and $W = c|E_0|^2/8\pi$ the incident optical power per unit area.

Figure 4 illustrates the calculated absorption rate associated to the spin-split surface states of the $\sqrt{3}$Pb/Ge(111) and the Rashba-like Au(111) surfaces. For $\sqrt{3}$Pb/Ge(111), the absorption spectrum is bounded in the 0.1–0.3 eV energy range, corresponding approximately to the spin splitting at the Fermi level. At this surface, the spectrum presents a prominent peak close to 0.17 eV, where the spin-flip absorption rate reaches a remarkable maximum value of 6%.

This result demonstrates that a significant part of the incoming radiation is dissipated exclusively in the spin-flip phenomena. The presence of SO coupling, which makes the orbital and spin degrees of freedom interrelated, causes a question on the angular momentum conservation. As the absorption of circularly polarized light induces a net transfer of angular momentum, the resulting magnetization of the surface states can produce a corresponding angular momentum reservoir in a SO-coupled system. Because of anisotropy of spin polarization (see Fig. 3), the absorption spectrum exhibits a substantial variation as a function of light polarization. As an example, close to 0.25 eV, the spin-flip absorption rate for L polarized light is approximately three times stronger than for R polarized light. In contrast, we find that the absorption spectrum of Au(111) is practically polarization independent. The reason is that this system exhibits an almost perfect isotropy, as assumed in the Rashba model. The magnitude of the spin-flip contribution for Au(111) is relatively weak (0.8% maximum). Thus, the spin-flip absorption in $\sqrt{3}$Pb/Ge(111) is 1 order of magnitude stronger in comparison to Au(111).

It is noteworthy that the bare spin-flip contribution to the absorption rate in $\sqrt{3}$Pb/Ge(111) is around three times stronger than the total absorption of a graphene layer (2.3%), where the electron spin does not play any significant role [33,34]. Thus, the *a priori* weaker relativistic SO interaction in $\sqrt{3}$Pb/Ge(111) exceeds the effect of the usually predominant nonrelativistic terms such as the electric dipole mechanism. The reason why the spin-flip contribution in this system is so important is that the hot spot matrix elements [Fig. 3(c)] lie just inside the Brillouin zone area where the S state is occupied and the S' state remains empty. In this way, the Fermi occupation factors allow electron transitions precisely where the matrix elements are maximal. From the discussion above, we can conclude that a large anomalous feature associated to the enhanced spin-flip excitation mechanism should be accessible by infrared optical spectroscopy in the 0.1–0.3 eV energy range.

In summary, we investigate the role of the SO interaction on the light absorption rate of the $\sqrt{3}$Pb/Ge(111) surface. Our calculations incorporate the full spinor wave function–structure from first principles, making use of a precise integration procedure through a Wannier interpolation scheme for the spin-flip matrix elements. We find that a substantial part of the low-energy absorption spectrum is dominated exclusively by the spin-flip excitations associated to the spin-polarized surface states. It is noteworthy that these transitions capture as much as 6% of the total incident power, representing an enhancement of 1 order of magnitude in comparison to the Rashba-like prototype Au(111) surface. The origin of such a huge absorption rate is closely related to the strong anisotropy exhibited by the spin-polarization structure connected to the surface states. As demonstrated in this Letter, a clear fingerprint of the spin-flip absorption mechanism should be accessible in the optical range, posing a challenge for further experimental work.

We acknowledge fruitful discussions with B. Rousseau, I. Errea, A. Kuzmenko, and R. Winkler. This work was supported by the UPV/EHU (Grant No. IT-366-07 and program UFI 11/55), the Spanish Ministry of Science

and Innovation (Grants No. FIS2010-19609-C02-00 and No. FIS2009-12773-C02-01), and the Basque Government (Grant No. IT472-10). The authors also acknowledge the Donostia International Physics Center (DIPC) for providing the computer facilities.

[1] C. L. Kane and E. J. Mele, Phys. Rev. Lett. **95**, 146802 (2005).
[2] S. Zhang and Z. Yang, Phys. Rev. Lett. **94**, 066602 (2005).
[3] J. I. Pascual, G. Bihlmayer, Y. M. Koroteev, H.-P. Rust, G. Ceballos, M. Hansmann, K. Horn, E. V. Chulkov, S. Blügel, P. M. Echenique *et al.*, Phys. Rev. Lett. **93**, 196802 (2004).
[4] A. Strozecka, A. Eiguren, and J. I. Pascual, Phys. Rev. Lett. **107**, 186805 (2011).
[5] J. B. Miller, D. M. Zumbühl, C. M. Marcus, Y. B. Lyanda-Geller, D. Goldhaber-Gordon, K. Campman, and A. C. Gossard, Phys. Rev. Lett. **90**, 076807 (2003).
[6] M. A. Leontiadou, K. L. Litvinenko, A. M. Gilbertson, C. R. Pidgeon, W. R. Branford, L. F. Cohen, M. Fearn, T. Ashley, M. T. Emeny, B. N. Murdin *et al.*, J. Phys. Condens. Matter **23**, 035801 (2011).
[7] O. Z. Karimov, G. H. John, R. T. Harley, W. H. Lau, M. E. Flatté, M. Henini, and R. Airey, Phys. Rev. Lett. **91**, 246601 (2003).
[8] M. Heide, G. Bihlmayer, P. Mavropoulos, A. Bringer, and S. Blügel, Psi-k Newsletter **78**, 1 (2006), http://www.psi-k.org/newsletters/News_78/Highlight_78.pdf.
[9] S. LaShell, B. A. McDougall, and E. Jensen, Phys. Rev. Lett. **77**, 3419 (1996).
[10] E. I. Rashba, Sov. Phys. Solid State **2**, 1109 (1960).
[11] E. I. Rashba and Y. A. Bychkov, JETP Lett. **39**, 79 (1984).
[12] A. Strozecka, A. Eiguren, and J. I. Pascual, Phys. Rev. Lett. **107**, 186805 (2011).
[13] A. Eiguren and C. Ambrosch-Draxl, New J. Phys. **11**, 013056 (2009).
[14] D. Sánchez-Portal, S. Riikonen, and R. M. Martin, Phys. Rev. Lett. **93**, 146803 (2004).
[15] I. Gierz, T. Suzuki, E. Frantzeskakis, S. Pons, S. Ostanin, A. Ernst, J. Henk, M. Grioni, K. Kern, and C. R. Ast, Phys. Rev. Lett. **103**, 046803 (2009).
[16] D. Khomitsky, J. Exp. Theor. Phys. **114**, 738 (2012).
[17] K. Sakamoto, T. Oda, A. Kimura, K. Miyamoto, M. Tsujikawa, A. Imai, N. Ueno, H. Namatame, M. Taniguchi, P. E. J. Eriksson *et al.*, Phys. Rev. Lett. **102**, 096805 (2009).
[18] J. Ibañez-Azpiroz, A. Eiguren, and A. Bergara, Phys. Rev. B **84**, 125435 (2011).
[19] M.-H. Liu and C.-R. Chang, Phys. Rev. B **80**, 241304 (2009).
[20] K. Yaji, Y. Ohtsubo, S. Hatta, H. Okuyama, K. Miyamoto, T. Okuda, A. Kimura, H. Namatame, M. Taniguchi, and T. Aruga, Nature Commun. **1**, 1 (2010).
[21] P. Tamarat, N. B. Manson, J. P. Harrison, R. L. McMurtrie, A. Nizovtsev, C. Santori, R. G. Beausoleil, P. Neumann, T. Gaebel, F. Jelezko *et al.*, New J. Phys. **10**, 045004 (2008).
[22] E. I. Rashba and A. L. Efros, Phys. Rev. Lett. **91**, 126405 (2003).
[23] E. Y. Sherman, Phys. Rev. B **67**, 161303 (2003).
[24] E. Frantzeskakis, S. Pons, and M. Grioni, Phys. Rev. B **82**, 085440 (2010).
[25] E. I. Blount, Solid State Phys. **13**, 305 (1962).
[26] X. Wang, J. R. Yates, I. Souza, and D. Vanderbilt, Phys. Rev. B **74**, 195118 (2006).
[27] I. Souza, N. Marzari, and D. Vanderbilt, Phys. Rev. B **65**, 035109 (2001).
[28] A. A. Mostofi, J. R. Yates, Y. Lee, I. Souza, D. Vanderbilt, and N. Marzari, Comput. Phys. Commun. **178**, 685 (2008).
[29] P. Giannozzi, S. Baroni, N. Bonini, M. Calandra, R. Car, C. Cavazzoni, D. Ceresoli, G. L. Chiarotti, M. Cococcioni, I. Dabo *et al.*, J. Phys. Condens. Matter **21**, 395502 (2009).
[30] A. DalCorso and A. MoscaConte, Phys. Rev. B **71**, 115106 (2005).
[31] D. M. Ceperley and B. J. Alder, Phys. Rev. Lett. **45**, 566 (1980).
[32] L. Kleinman and D. M. Bylander, Phys. Rev. Lett. **48**, 1425 (1982).
[33] V. P. Gusynin, S. G. Sharapov, and J. P. Carbotte, Phys. Rev. Lett. **96**, 256802 (2006).
[34] A. B. Kuzmenko, E. van Heumen, F. Carbone, and D. van der Marel, Phys. Rev. Lett. **100**, 117401 (2008).
[35] K. Anton, Comput. Mater. Sci. **28**, 155 (2003).